



This paper is a part of the hereunder thematic dossier published in OGST Journal, Vol. 69, No. 3, pp. 379-499 and available online [here](#)

Cet article fait partie du dossier thématique ci-dessous publié dans la revue OGST, Vol. 69, n°3 pp. 379-499 et téléchargeable [ici](#)

DOSSIER Edited by/Sous la direction de : J.-F. Argillier

IFP Energies nouvelles International Conference / Les Rencontres Scientifiques d'IFP Energies nouvelles
Colloids 2012 – Colloids and Complex Fluids: Challenges and Opportunities
Colloids 2012 – Colloïdes et fluides complexes : défis et opportunités

Oil & Gas Science and Technology – Rev. IFP Energies nouvelles, Vol. 69 (2014), No. 3, pp. 379-499

Copyright © 2014, IFP Energies nouvelles

- 379 >Editorial
H. Van Damme, M. Moan and J.-F. Argillier
- 387 >Formation of Soft Nanoparticles via Polyelectrolyte Complexation: A Viscometric Study
Formation de nanoparticules molles par complexation de polyélectrolytes : une étude viscosimétrique
C. Rondon, J.-F. Argillier, M. Moan and F. Leal Calderon
- 397 >How to Reduce the Crack Density in Drying Colloidal Material?
Comment réduire la densité de fractures dans des gels colloïdaux ?
F. Boulogne, F. Giorgiutti-Dauphiné and L. Pauchard
- 405 >Adsorption and Removal of Organic Dye at Quartz Sand-Water Interface
Adsorption et désorption d'un colorant organique à l'interface sable de quartz-eau
A. Jada and R. Ait Akbour
- 415 >Freezing Within Emulsions: Theoretical Aspects and Engineering Applications
Congélation dans les émulsions : aspects théoriques et applications techniques
D. Clausse and C. Dalmazzone
- 435 >Effect of Surfactants on the Deformation and Detachment of Oil Droplets in a Model Laminar Flow Cell
Étude de l'effet de tensioactifs sur la déformation et le détachement de gouttes d'huiles modèles à l'aide d'une cellule à flux laminaire
V. Fréville, E. van Hecke, C. Ernenwein, A.-V. Salsac and I. Pezron
- 445 > Investigation of Interfacial Phenomena During Condensation of Humid Air on a Horizontal Substrate
Investigation de phénomènes interfaciaux au cours de la condensation d'air humide sur un substrat horizontal
A. Tiwari, J.-P. Fontaine, A. Kondjoyan, J.-B. Gros, C. Vial and C.-G. Dussap
- 457 > Microfluidic Study of Foams Flow for Enhanced Oil Recovery (EOR)
Étude en microfluidique de l'écoulement de mousses pour la récupération assistée
N. Quennouz, M. Ryba, J.-F. Argillier, B. Herzhaft, Y. Peysson and N. Pannacci
- 467 > Non-Aqueous and Crude Oil Foams
Mousses non aqueuses et mousses pétrolières
C. Blázquez, É. Emond, S. Schneider, C. Dalmazzone and V. Bergeron
- 481 > Development of a Model Foamy Viscous Fluid
Développement d'un modèle de dispersion gaz-liquide de type mousse liquide visqueuse
C. Vial and I. Narchi
- 499 > Erratum
D.A. Saldana, B. Creton, P. Mougín, N. Jeuland, B. Rousseau and L. Starck

Development of a Model Foamy Viscous Fluid

C. Vial^{1,2*} and I. Narchi³

¹ Clermont Université, Université Blaise Pascal, Institut Pascal, Campus des Cézeaux, Bâtiment Polytech, 24 avenue des Landais, BP 20206, 63174 Aubière Cedex - France

² CNRS, UMR 6602, CNRS, IP, 63171 Aubière - France

³ Mars GmbH, Eitzer Strasse 215, 27283 Verden - Germany
e-mail: christophe.vial@univ-bpclermont.fr - issa.narchi@effem.com

* Corresponding author

Résumé — Développement d'un modèle de dispersion gaz-liquide de type mousse liquide visqueuse —

L'objectif est de développer un fluide modèle représentatif des « mousses liquides », c'est-à-dire présentant un taux de vide en deçà de l'empilement aléatoire de sphères, dont les propriétés rhéologiques et la stabilité peuvent être prédites. Tout d'abord, la préparation de ces fluides modèles sera décrite à la fois en termes de formulation et de procédés. Ensuite, les résultats expérimentaux seront discutés. Ceux-ci montrent que des mousses liquides visqueuses modèles présentant une distribution de tailles de bulles monomodales ont été obtenues avec un taux de vide entre 25 % et 50 % (v/v). Leurs propriétés viscoélastiques en écoulement et aux faibles déformations résultent des interactions entre la formulation de la phase continue, le taux de vide et le diamètre des bulles. Leur viscosité apparente peut être décrite par un modèle de Cross et la viscosité à cisaillement nul peut être prédite par le modèle de Mooney jusqu'à un taux de gaz de 40 %. Les mesures en mode harmonique ont montré que les règles de Cox-Merz et de Laun s'appliquent quand le nombre capillaire Ca est inférieur à 0,1. L'étendue du plateau Newtonien à faible cisaillement décroît lorsque le taux de vide augmente ou lorsque la taille des bulles diminue. Dans le domaine rhéofluidifiant, la contrainte de cisaillement varie proportionnellement à $Ca^{1/2}$, comme dans les mousses humides présentant des interfaces immobilisées. Finalement, les mousses liquides visqueuses obtenues ont pu être cisailées jusqu'à des valeurs de Ca de 0,1 sans modifier leur microstructure. La stabilité de ces fluides au repos atteint plusieurs heures et elle augmente avec le taux de vide à cause des contraintes stériques entre les bulles ; ils constituent donc des fluides modèles intéressants pour l'étude des mousses liquides visqueuses présentant un taux de vide en deçà de l'empilement aléatoire de sphères.

Abstract — Development of a Model Foamy Viscous Fluid — The objective is to develop a model viscous foamy fluid, i.e. below the very wet limit, the rheological and stability properties of which can be tuned. First, the method used for the preparation of foamy fluids is detailed, including process and formulation. Then, experimental results highlight that stable foamy fluids with a monomodal bubble size distribution can be prepared with a void fraction between 25% and 50% (v/v). Their viscoelastic properties under flow and low-strain oscillatory conditions are shown to result from the interplay between the formulation of the continuous phase, void fraction and bubble size. Their apparent viscosity can be described using the Cross equation and zero-shear Newtonian viscosity may be predicted by a Mooney equation up to a void fraction about 40%. The Cox-Merz and the

Laun's rules apply when the capillary number Ca is lower than 0.1. The upper limit of the zero-shear plateau region decreases when void fraction increases or bubble size decreases. In the shear-thinning region, shear stress varies with $Ca^{1/2}$, as in wet foams with immobile surfaces. Finally, foamy fluids can be sheared up to Ca about 0.1 without impairing their microstructure. Their stability at rest achieves several hours and increases with void fraction due to compact packing constraints. These constitute, therefore, versatile model fluids to investigate the behaviour of foamy fluids below the very wet limit in process conditions.

NOMENCLATURE

d_i	Bubble diameter (m)
d_{43}	Volume-average bubble diameter (m)
\bar{d}	Number-average bubble diameter (m)
D_S	Surface diffusion coefficient ($\text{m}^2 \cdot \text{s}^{-1}$)
E_S	Interfacial elasticity ($\text{N} \cdot \text{m}^{-1}$)
f	Viscosity function
f_i	Number fraction of spheres of diameter d_i
g	Acceleration of gravity ($\text{m} \cdot \text{s}^{-2}$)
G^*	Complex shear modulus (Pa)
G'	Storage modulus (Pa)
G''	Loss modulus (Pa)
$h(t)$	Liquid height (m)
h_0	Beaker height in destabilization experiments (m)
k_B	Constant of the modified Barnea-Mizrahi model
k_C	Constant of the Cross model
m	Cross model exponent
N_1	Primary normal stress difference (Pa)
N_2	Secondary normal stress difference (Pa)
Q_c	Flow rate of the continuous phase ($\text{m}^3 \cdot \text{s}^{-1}$)
Q_d	Flow rate of the dispersed phase ($\text{m}^3 \cdot \text{s}^{-1}$)
R_{32}	Bubble Sauter mean radius (m)
S	Destabilization parameter (%)
t	Time (s)
v_b	Bubble rise velocity in the foamy fluid ($\text{m} \cdot \text{s}^{-1}$)
v_∞	Terminal rise velocity of a single bubble ($\text{m} \cdot \text{s}^{-1}$)

GREEK LETTERS

α, β	Dimensionless constants
γ	Shear strain
$\dot{\gamma}$	Shear rate (s^{-1})
δ	Phase angle ($^\circ$)
δd	Difference between bubble diameter and number-average bubble diameter (m)
$\Delta\rho$	Density difference between continuous and dispersed phases ($\text{kg} \cdot \text{m}^{-3}$)
ϕ	Void fraction

ϕ_m	Maximum packing fraction of spherical bubbles
η	Viscosity of the foamy fluid (Pa.s)
η^*	Complex viscosity of the foamy fluid (Pa.s)
η_c	Viscosity of the continuous phase (Pa.s)
η_0	Zero-shear viscosity (Pa.s)
η_∞	Infinite-shear viscosity (Pa.s)
κ	Viscosity ratio
ρ	Density of the foamy fluid ($\text{kg} \cdot \text{m}^{-3}$)
ρ_c	Density of the continuous phase ($\text{kg} \cdot \text{m}^{-3}$)
ρ_d	Density of the dispersed phase ($\text{kg} \cdot \text{m}^{-3}$)
σ	Surface tension ($\text{N} \cdot \text{m}^{-1}$)
τ	Shear stress (Pa)

DIMENSIONLESS NUMBERS

Ca	Capillary number
Fr	Froude number
Ma	Marangoni number
Pe	Péclet number
Re	Reynolds number

INTRODUCTION

Foamy fluids constitute a particular class of gas-liquid dispersions that has been disregarded in the recent literature in comparison to foams or to conventional bubbly flows. In the oil and gas industry, they have gained interest only in the 90s because of the “foamy oil phenomenon” that causes higher production rates than expected for unconventional oil reservoirs, as this phenomenon could be explained by the particular viscosity behavior of foamy fluids. In practice, conventional bubbly flows have been extensively studied since the 70s, in the presence or in the absence of tensioactive agents in the liquid phase (see, e.g., Camarasa *et al.*, 1999). Conventional bubbly flows cover the situation where a gas phase is dispersed in forms of bubbles of various shapes (spherical,

ellipsoidal but also spherical caps, etc.) in a low-viscosity aqueous solution (Ruzicka *et al.*, 2003) or in an organic liquid (Chaumat *et al.*, 2007). They can be observed only under flow conditions, are characterized by a gas volume fraction ϕ usually lower than 25% (also denoted void fraction), are mainly driven by bubble-bubble interactions known to play a key role when ϕ is above 5% and are usually modeled as turbulent flows (Ekambara *et al.*, 2008). They are encountered first in the chemical and petrochemical industries to carry out oxidation, hydrogenation and chlorination reactions, in biochemical fermentations and in water treatment processes in which the gas dispersion is produced mechanically, pneumatically or using the kinetic energy of the liquid phase (Gourich *et al.*, 2008). They are also common in gas, coal and nuclear power plants in which the dispersion is produced by the nucleate boiling process (Hibiki *et al.*, 2006). In parallel, the physics of foams has been extensively investigated since the pioneering works of H.M. Princen in the 80s (Weaire and Hutzler, 1999), in particular their complex rheological properties exhibiting a viscoelastoplastic behavior (Herzhaft, 1999; Weaire, 2008). These are considered as the simplest example of soft condensed matter. Foams are commonly divided into dry foams ($\phi \geq 99\%$) in which bubbles are polyhedral, and wet foams ($64\% \leq \phi \leq 99\%$) in which bubbles progressively approach a spherical shape when ϕ decreases. A summary of the recent research on their yield stress and viscous friction is provided by Denkov *et al.* (2012), with a special focus on the key role of surfactants on the surface mobility of the bubbles by Politova *et al.* (2012).

As mentioned above, less attention has been paid to foamy fluids, *i.e.* below the very wet limit: as $\phi \leq 64\%$, these are not intrinsically “true” foams because of the reduced packing constraints, so that they exhibit no yield stress. However, they also differ from the conventional gas-liquid dispersions found in bubbly flows because they are constituted by a viscous or viscoelastic continuous matrix which stabilizes the dispersed phase in form of tiny spherical bubbles exhibiting colloidal interactions with the matrix. Figure 1 highlights the differences between the respective bubble topologies at rest: spherical in foamy fluids, slightly deformed spheres in wet foams and “deformed ellipsoidal” in conventional air-water bubbly flows. Foamy fluids cover many typical industrial situations, such as foamed cement (Ahmed *et al.*, 2009), foamy oils (Abivin *et al.*, 2009) or food foams (Murray *et al.*, 2011) but they also describe bubbles in magma (Pal, 2003). Even though the presence of foaming agents adsorbed at the interface is often required to delay bubble coalescence, the role of interfacial properties is reduced in comparison to wet or dry

foams because it is counterbalanced by the influence of the bulk properties (mainly viscosity) and the role of the microstructure of the continuous phase, such as the partial coalescence of fat in whipped cream (Hotrum *et al.*, 2005).

Foamy fluids are often compared to emulsions and treated as concentrated emulsions of bubbles, as the rheology of concentrated emulsions has been more deeply investigated and reviewed in the literature (*e.g.*, Derkach, 2009). However, the rheology of foamy fluids may significantly differ from that of concentrated emulsions. For example, depending on gas volume fraction and the interactions between the adsorbed layers and the microstructure in the bulk, the apparent viscosity of foamy fluids may be higher or lower than that of its continuous phase, which is never reported for emulsions (Pal, 2006). This specific behavior has been already observed in foamy oils (Abivin *et al.*, 2009), but also in aerated foods in which the gas phase can make the matrix softer or more consistent (Thakur *et al.*, 2008). As a conclusion, the rheology and the properties of foamy fluids remain far less understood than those of emulsions and foams. This is reinforced by a lack of experimental results. For example, rheological data remains scarce on bubbles in magma for which they are limited either to very high viscosity values for the continuous phase (above 50 Pa.s for Llewellyn *et al.*, 2002) or to moderate void fraction ($\phi < 17\%$ for Rust and Manga, 2002) but always without any surfactant. Similarly, rheological data is scarce on foamy oils in which asphaltenes seem to play a tensioactive role (Abivin *et al.*, 2009; Wang *et al.*, 2009), and on aerated food products because of proteins: a typical example is whipped cream for which data on rheology, void fraction and bubble size can hardly be found simultaneously except in a few papers (*e.g.*, Jakubczyk and Niranjani, 2006). Finally, further work is still needed to better understand the underlying physics of the rheology of foamy fluids.

The objective of the present paper is, therefore, to develop a model foamy fluid, the rheological and stability properties of which can be tuned and predicted, so that it can be used to investigate more deeply the rheology of foamy fluids, first from a theoretical point of view, but also in their industrial applications, such as foamy oils. First, the method used for the production of the continuous and the dispersed phases will be detailed. Then, the stability over time and the rheology of the foamy fluids will be investigated experimentally as a function of the preparation procedure, with the aim to establish predictive models. For this reason, the theoretical background on the rheology of dispersions and suspensions will be reviewed first.

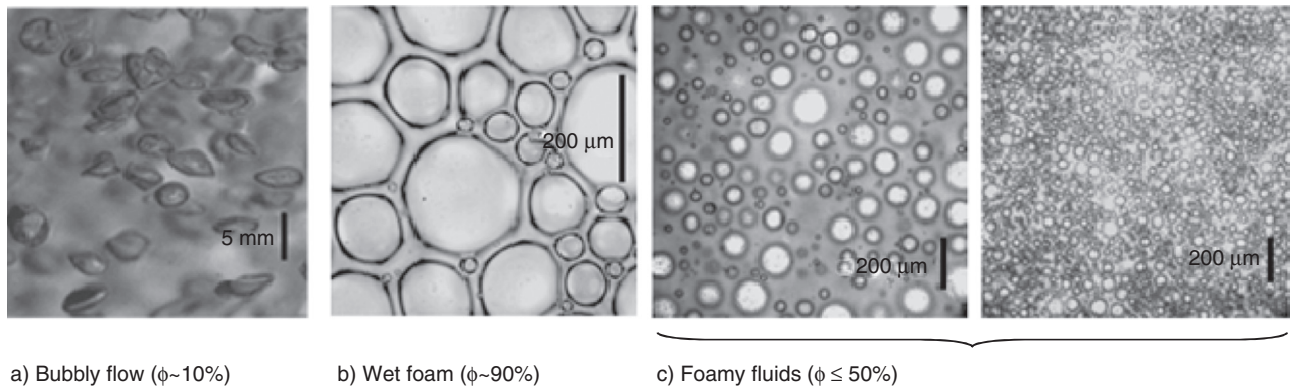


Figure 1

Examples of gas-liquid dispersions corresponding to conventional bubbly flows, wet foam and foamy fluids, respectively.

1 THEORETICAL BACKGROUND

The rheology of dilute, semi-dilute and concentrated foamy fluids using a Newtonian fluid as the continuous phase has retained less attention than that of non-colloidal and colloidal emulsions or suspensions of spherical particles. However, similar models have often been applied, neglecting the compressibility of the gas phase. For very dilute systems, the Taylor equation applies to bubbles with clean interfaces at low shear. This equation assumes that the suspension is Newtonian at low shear and gives access to the zero-shear viscosity (η_0) as a function of void fraction ϕ and of the viscosity of the continuous phase (η_c), as follows:

$$\eta_0 = \eta_c \left[1 + \frac{2 + 5\kappa}{2(1 + \kappa)} \phi \right] \quad \eta_0 \xrightarrow{\kappa \rightarrow 0} \eta_c [1 + \phi]$$

$$\eta_0 \xrightarrow{\kappa \rightarrow \infty} \eta_c \left[1 + \frac{5}{2} \phi \right] \quad (1)$$

In Equation (1), κ is the viscosity ratio between the dispersed and the continuous phases. κ is lower than 10^{-5} for bubbles in viscous fluids in this work. For this reason, it is usually assumed that κ tends towards 0 for bubbles in viscous fluids in the literature. Actually, this ratio measures to which extent the shear stress in the continuous phase is transmitted into the dispersed phase at the interface, but only for mobile interfaces. As a result, bubbles with interfaces rigidified by surfactants or any surface-active agent may behave as solid particles in terms of interface mobility, so that the tangential viscous stresses at the interface may vanish in the dispersed phase. The consequence is that for rigid interfaces, η_0 values may correspond to those obtained when $\kappa \rightarrow \infty$ in Equation (1) even if $\kappa \rightarrow 0$ in practice.

Extensions to semi-dilute systems involve higher order approximations, such as those developed by [Choi and Schowalter \(1975\)](#):

$$\eta_0 \xrightarrow{\kappa \rightarrow 0} \eta_c \left[1 + \frac{(4 - 10\phi^{7/3})\phi}{4 - 10\phi + 10\phi^{7/3} - 4\phi^{10/3}} \right]$$

$$\eta_0 \xrightarrow{\kappa \rightarrow \infty} \eta_c \left[1 + \frac{10(1 - \phi^{7/3})\phi}{4 - 25\phi + 42\phi^{5/3} - 25\phi^{7/3} + 4\phi^{10/3}} \right] \quad (2)$$

or [Yaron and Gal-Or \(1972\)](#):

$$\eta_0 \xrightarrow{\kappa \rightarrow 0} \eta_c \left[1 + \frac{22\phi}{10(1 - \phi)} \right]$$

$$\eta_0 \xrightarrow{\kappa \rightarrow \infty} \eta_c \left[1 + \frac{(11/2) \cdot (10 + 4\phi^{7/3} - (84/11)\phi^{2/3})}{10(1 - \phi^{10/3}) - 25\phi(1 - \phi^{4/3})} \phi \right] \quad (3)$$

Alternative models developed until the late 90s have been reviewed by [Llewellyn et al. \(2002\)](#). More complex approaches take more accurately into account:

- the mobility of the interface which depends on the presence of adsorbed compounds able to promote either surface tension gradients or surface viscoelasticity;
- the order of magnitude of the interfacial, inertia, buoyancy and viscous forces, in particular their influence on bubble deformation under flow conditions.

The respective influence of these phenomena can be estimated using the dimensionless quantities defined in [Table 1](#): namely, the Reynolds (Re), capillary (Ca), Froude (Fr), surface Péclet (Pe) and Marangoni (Ma) numbers. Using the typical values of the shear rate ($\dot{\gamma}$) applied and of the Sauter mean radius (R_{32}) measured

TABLE 1
Typical values of the dimensionless numbers describing the phenomena involved in foamy fluids and their values in this work in the conditions of rheological testing

Dimensionless number	Ratio	Values in this work
$Re = \frac{\rho_c \dot{\gamma} (2R_{32})^2}{\eta_c}$	Inertia / viscous force	$Re \leq 10^{-6}$
$Ca = \frac{\eta_c \dot{\gamma} R_{32}}{\sigma}$	Viscous / surface force	$Ca \leq 1$
$Fr = \dot{\gamma} \sqrt{\frac{\rho_c R_{32}}{\Delta \rho g}} \approx \dot{\gamma} \sqrt{\frac{R_{32}}{g}}$	Inertia / buoyancy force	$10^{-6} \leq Fr \leq 1$
$Pe = \frac{\dot{\gamma} R_{32}^2}{D_S}$	Surface convection / diffusion	$Pe \gg 1$
$Ma = \frac{E_S R_{32}}{2\eta_c D_S}$	Surface elasticity / diffusion	$Ma >> 1$

in this work, Table 1 shows that viscous forces prevail over inertia, which corresponds to creeping flows. Buoyancy forces cannot be neglected at low shear, which highlights that foamy fluids will be unstable at rest and that bubbles will only exhibit a kinetic stability against gravity resulting from the high viscosity of the continuous phase. The capillary number measures the influence of viscous forces under steady flow conditions (Llewellyn *et al.*, 2002), as used in this work. Ca values show that surface forces predominate, except at high shear rate when interfacial effects and viscous forces achieve the same order of magnitude. It must however be mentioned that, even at intermediate Ca values, bubbles may undergo deformation, which may drastically modify the viscosity of the foamy fluid (Pal, 2006). η_0 can be estimated, therefore, using first-order deformation models that account only for Ca. However, this approach constitutes only a rough approximation, as it does not account for surface elasticity that can have a greater impact than surface tension on η_0 , especially in the presence of proteins.

At the level of the air/water interface, proteins are known to diffuse slowly in water, with a diffusivity about $10^{-10} \text{ m}^2 \cdot \text{s}^{-1}$ (Jung and Ebeleer, 2003), which gives an order of magnitude of $10^{-13} \text{ m}^2 \cdot \text{s}^{-1}$ for the diffusivity in the foamy fluid on the basis of the Stokes-Einstein equation. This suppresses the tangential mobility of the adsorbed compounds and the Marangoni effect, which is highlighted by the elevated Pe values. But proteins also promote surface elasticity that induces interface immobilization, emphasized by the high Ma value, as surface elasticity (E_S) is about $30 \times 10^{-3} \text{ N} \cdot \text{m}^{-1}$ for whey

proteins at air/water interfaces as used in this work (Marinova *et al.*, 2009). This modifies drastically the rheology of wet foams (Denkov *et al.*, 2005), even though the influence of surface elasticity on foamy fluids is still to be investigated. As a conclusion, bubble interfaces may be considered as partially or totally immobilized in this work.

For low Ca values, Pal (2011) developed a generalized approach able to describe the zero-shear viscosity of concentrated emulsions which is based on those suggested in Pal (2003) for bubbles in magma. This can be expressed using the viscosity of the continuous phase (η_c) and a viscosity function (f), as follows:

$$\left(\frac{\eta_0}{\eta_c}\right)^\alpha = f(\phi, \phi_m) \quad (4)$$

with $\alpha = 1$ for rigidified interfaces and $\alpha = 5/2$ for clean mobile interfaces. In this equation, ϕ_m is the maximum packing fraction of the spherical bubbles. Several $f(\phi, \phi_m)$ functions, depending only on the void fraction $\phi \leq \phi_m$, have been proposed in the literature. They describe the extent of the packing constraints, *i.e.* the difficulty to add a volume fraction $d\phi$ of bubbles in a foamy fluid with a void fraction $\phi \leq \phi_m$. They are summarized in Table 2 in which Equation (5a), (5b) and (5c) correspond to the Brinkman-Roscoe, Mooney and Krieger-Dougherty models, respectively (Pal, 2011).

For spherical bubbles assumed to be rigid and monodisperse, common ϕ_m values are 0.637 for close random packing and 0.74 for the thickest regular packing. For foamy fluids, the random packing value seems more

TABLE 2
Example of viscosity functions for concentrated emulsions and bubbly suspensions

Example of $f(\phi, \phi_m)$ values proposed by Pal (2011) in Equation (4) at low Ca values		
$\left(1 - \frac{\phi}{\phi_m}\right)^{\frac{5}{2}}$ (5a)	$\exp\left(\frac{5}{2}\phi / \left(1 - \frac{\phi}{\phi_m}\right)\right)$ (5b)	$\left(1 - \frac{\phi}{\phi_m}\right)^{\frac{5}{2}\phi_m}$ (5c)

accurate but it is also well-known that polydispersity increases ϕ_m . Pal (2003) suggested that ϕ_m should be estimated using an Ouchiya and Tanaka formulation in which f_i is the number fraction of spheres of diameter d_i :

$$\phi_m = \frac{\sum f_i d_i^3}{\sum f_i \cdot \delta d^3 + \beta^{-1} \cdot \sum f_i [(d_i + \bar{d})^3 - \delta d^3]} \quad (6a)$$

with $\delta d = \max [(d_i - \bar{d}); 0]$

$$\beta = 1 + \frac{4}{13} (8 \cdot 0.637 - 1) \bar{d} \frac{\sum f_i (d_i + \bar{d})^2 \left[1 - \frac{(3/8)\bar{d}}{d_i + \bar{d}} \right]}{\sum f_i [d_i^3 - \delta d^3]}$$

with $\bar{d} = \sum f_i d_i$

(6b)

An alternative solution is the Quemada model (Berli and Quemada, 2000), an effective approach for concentrated particle suspensions exhibiting colloidal interactions, that has also been applied successfully to represent the viscosity of colloidal emulsions. At low Ca, this provides a relation similar to Equation (5c) with $\phi_m = 4/5$:

$$\eta_0 = \eta_c \left(1 - \frac{\phi}{\phi_m} \right)^{-2} \quad (7)$$

This kind of approach was criticized by Llewellyn and Manga (2005), arguing that due to bubble deformation, ϕ_m values based on a spherical shape had no physical meaning, so that $\phi_m = 1$ should be applied. This contradicts, however, the results from Saint-Jalmes and Durian (1999) who determined that foam elasticity vanished when ϕ was 0.64 and justified that viscosity models below and above ϕ_m should differ. This statement agrees with the earlier results from the literature reviewed by these authors.

However, all the above-mentioned models apply only for small deformation, *i.e.* low shear and low capillary number. They all consider that bubble size has no effect on viscosity. At intermediate Ca values, when bubble deformation may become high, zero-order models usually fail. Empirical models have sometimes been applied, such as a simplified version of the Cross model that introduces Ca in the evolution of the viscosity of the foamy fluid (η). These usually account for a zero-shear viscosity value (η_0) derived from the zero-order models described previously to account for the fluid behaviour at low shear (*e.g.*, Rust and Manga, 2002):

$$\eta = \frac{\eta_0}{1 + (k_C Ca)^m} \quad (8)$$

Some rheological models including an infinite shear viscosity η_∞ with $\eta < \eta_c$ have also been applied but the

presence of a Newtonian plateau region at high shear is not ascertained in this work due to the possible changes of flow topology. In practice, η_∞ has hardly been observed experimentally in the literature, except for highly viscous continuous phases coupled with high ϕ values (*e.g.*, Llewellyn *et al.*, 2002). In parallel, more fundamental approaches have been developed on the basis of a first-order approximation. For example, a simplified version of the Barthel-Biesel & Chim model for viscoelastic deformable objects has been suggested to describe the behaviour of foamed cements under flow by Ahmed *et al.* (2009):

$$\eta = \eta_c [1 + (2.5 - 70 \cdot Ca^2) \phi] \quad (9)$$

However, this model is valid only for $Ca \leq 0.2$ and it does not fit the data from Llewellyn *et al.* (2002). Alternative analytical solutions for intermediate Ca values based on a first-order deformation or for higher Ca values, as suggested by Rust and Manga (2002) for foamy fluids, include the Frankel and Acrivos model for dilute systems with $\kappa = 0$

$$\eta = \eta_c \left[1 + \frac{1 - (12/5)Ca^2}{1 + (6Ca/5)^2} \phi \right] \quad (10)$$

and the Han and King approach for semi-dilute systems, also with $\kappa = 0$:

$$\eta = \eta_c \left[\frac{1 + (6Ca/5)^2 (1 + (20/3)\phi)(1 + 4\phi)}{1 + (6Ca/5)^2 (1 + (20/3)\phi)^2} \right] \times \left(1 + \phi + \frac{5}{2} \phi^2 \right) \quad (11)$$

One can point out that these equations, under simple shear flow, are similar to those obtained with emulsions, although they account for the dilatational viscosity and the compressibility of the dispersed phase (Pal, 2006). These models predict, in agreement with the literature data, that the foamy fluids exhibit viscoelastic properties under flow even when the continuous phase is Newtonian. For Equation (10), the corresponding values of the normal stress differences N_1 and N_2 are expressed as:

$$N_1 = \left(\frac{\sigma}{R_{32}} \right) \frac{32/5}{1 + (6Ca/5)^2} \phi Ca^2 \quad (12)$$

$$-N_2 = \frac{16/5}{1 + (6Ca/5)^2} \left(\frac{\sigma}{R_{32}} \right) \left[1 - 3 \frac{1 + (6Ca/5)^2}{28} \right] \phi Ca^2$$

while the calculations yield nearly the same expression for N_1 using the Han and King approach with a second order approximation on ϕ (Vinckier *et al.*, 1999):

$$N_1 = \left(\frac{\sigma \eta_c}{R_{32} \eta} \right) \frac{32/5}{1 + (6Ca/5)^2} Ca^2 \phi \left(1 + \phi + \frac{5}{2} \phi^2 \right) \quad (13)$$

All these models predict that N_1 and N_2 tend to 0 when ϕ tends towards 0.

For bubble-concentrated magmas, Pal (2003) suggested a modified version of Equation (4), valid for bubbles with mobile interfaces ($\alpha = 5/2$ in Eq. 4). This accounts for the Frankel and Acrivos model and for the viscosity functions $f(\phi, \phi_m)$ summarized in Table 2:

$$\left(\frac{\eta}{\eta_c} \right) \left[\frac{1 - (12/5)Ca^2(\eta/\eta_c)^2}{1 - (12/5)Ca^2} \right]^{-4/5} = [f(\phi, \phi_m)]^{1/2} \quad (14)$$

Equations (9-11) and (14) present the advantage to predict that $\eta \leq \eta_c$ for intermediate and high Ca values, which is in agreement with the experimental data of Rust and Manga (2002), Ahmed *et al.* (2009) and Abivin *et al.* (2009). Equations (10-11) and (14) also predict that the influence of Ca on η always vanishes when $Ca > 10$. However, this should not necessarily fit experimental data, as spherical bubbles may undergo deformation that can no more be described using first-order models when Ca is higher than 1. Concerning viscoelasticity, these models predict that N_1 and N_2 tend towards 0 when $Ca \rightarrow 0$, as expected, and that they increase steeply with Ca until Ca is about 1. They also predict that N_1 tends towards a constant and that $|N_2|$ varies as Ca^2 when $Ca \rightarrow \infty$ but these first-order models should not apply in this range of Ca values.

Figure 2a illustrates the comparison of zero-order models for η_0 reported in this short review of the literature. This highlights that there is a large discrepancy between the η_0 values predicted by the rheological models applied to foamy fluids. This stems, first, from the rigidity of the interface that can be modelled using either the α constant of Equation (4) or the viscosity ratio κ which can be artificially increased to account for interface immobilization. However, the zero-shear viscosity predicted for concentrated systems is also highly dependent on the assumptions on the modelling of the packing constraints that differ in the literature (Eq. 5) and on the value of the maximum packing parameter ϕ_m . Figure 2b quantifies the influence of Ca on the viscosity of the foamy fluid at constant $\phi = 0.5$ and $\phi = 0.637$ values. The same discrepancy as in Figure 2a emerges on η_0 at low Ca but the models usually agree when they predict that viscous forces have a significant effect only when

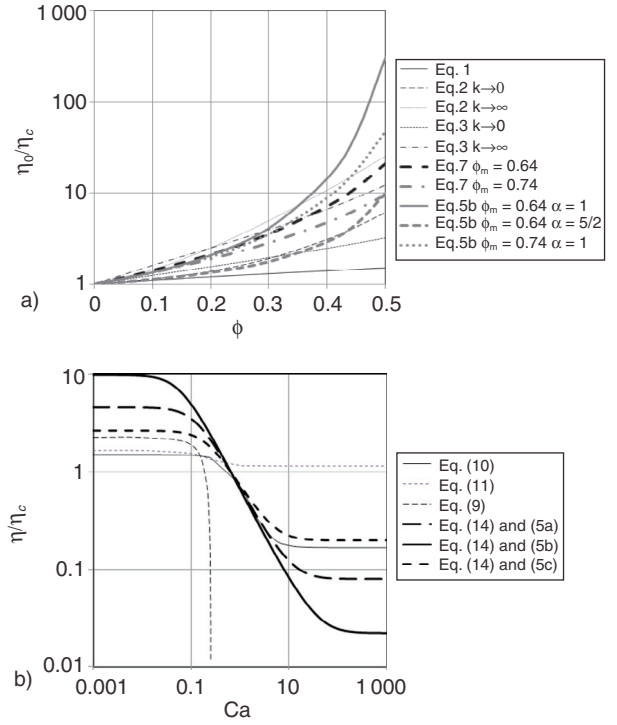


Figure 2

a) Predictions of the zero-shear viscosity (η_0) as a function of ϕ , ϕ_m and α for different models. b) Predictions of the foamy fluid viscosity (η) as a function of Ca for $\phi = 0.5$, $\phi_m = 0.637$ and various models.

$Ca > 0.1$, except for Equation (9) for which the steep evolution is limited in the range $0.1 \leq Ca \leq 0.2$. One can also point out that all equations predict that $\eta/\eta_c \leq 1$ when $Ca \rightarrow \infty$ in Figure 2b, except Equation (11). Similarly, all these models predict that η/η_c is a decreasing function of ϕ at high Ca , again except Equation (11) (data not shown). This means that η_0/η_c increases with ϕ at very low Ca , while the opposite trend emerges usually at high Ca , highlighting a key effect of the gas phase. For Equation (11), one obtains $\eta/\eta_c \leq 1$ only for $\phi \leq 0.2$; consequently, this model disagrees with most of experimental data from the literature, for example with those from Llewellyn *et al.* (2002) which showed that the ratio η/η_c was lower than 1 at high Ca and decreased when ϕ increased.

2 MATERIALS AND METHODS

Foamy fluids were prepared by mixing in water dehydrated glucose syrup for the viscous matrix with 2% (w/w) Whey Proteins Isolate (WPI) as the foaming

agent. Glucidex IT21 (*Roquette Frères*, France) was retained because of its low dextrose equivalent value of 21% (describing the degree of conversion of starch to dextrose), while ProLacta90 (*Lactalis*, France) was chosen for WPI. This mixture provided a Newtonian viscous aqueous phase, the viscosity (η_c) of which could be varied between 0.1 and 10 Pa.s as a function of the glucose syrup concentration. Polyacrylamide (PAAm) from *BHD. Lab. Suppliers* (UK) with a weight average molecular mass of 5×10^6 kDa was used as a rheology modifier so as to add a viscoelastic character. The advantage of this recipe was that viscosity (η_c) and viscoelasticity could be tuned independently by adjusting simultaneously the amount of glucose syrup and PAAm. The rheological properties and foamability of these formulations were investigated by *Narchi et al.* (2009). These authors showed that the PAAm-WPI-glucose syrup mixture still exhibited a constant viscosity *versus* shear rate when PAAm content remained 0.01% w/v (value used in this work), as a Newtonian fluid, but with a measurable normal force, as for a Boger fluid. They also showed that the presence of a foaming agent was compulsory due to the effect of the viscosity of the continuous phase: increasing viscosity impaired the maximum ϕ values that could be achieved. In addition, surface tension (σ) was nearly constant, as only whey proteins were used as a foaming agent. In this work, σ was measured using a K12 tensiometer (*Krüß GmbH* Germany) and the Wilhelmy plate method.

Foamy fluids were prepared using a continuous production line in which air and the continuous phase were injected concurrently. The gas phase was dispersed using a mixing head equipped with three four-blade right angle paddles (*Fig. 3*). Experiments were carried out at 20°C and atmospheric pressure. Further information on the experimental set-up can be found in *Narchi et al.* (2009, 2011). The rotation speed of the rotor could be varied but void fraction was modified mainly by varying gas flow rate. Under steady state conditions, the maximum void fraction that can be achieved may be derived from the values of the flow rates of the continuous (Q_c) and the dispersed (Q_d) phases under atmospheric pressure. This imposes the following constraint:

$$\phi \leq \frac{Q_d}{Q_c + Q_d} \quad (15)$$

Equality in Equation (15) means that all the gas phase is totally dispersed and stabilized in the form of tiny bubbles. The advantage of the continuous process was that void fraction and bubble size could be better controlled so as to improve reproducibility. Values of the Reynolds number based on the mixer diameter between 5 and 10

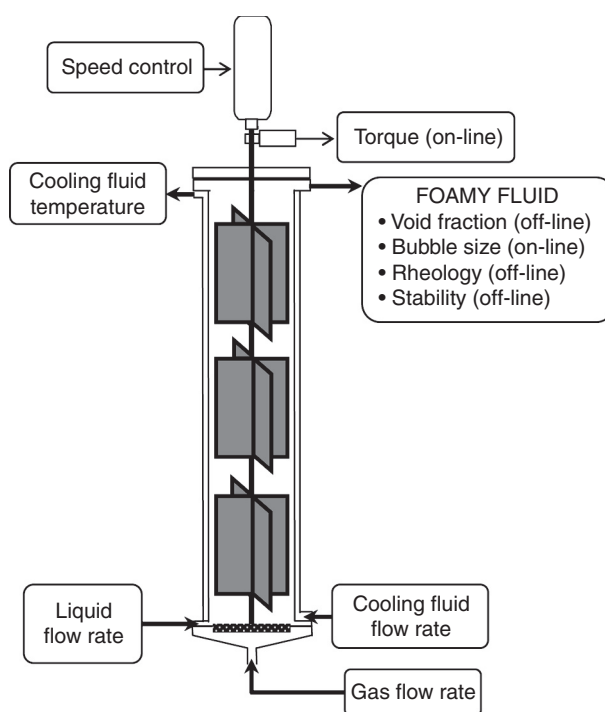


Figure 3

Schematic representation of the experimental set-up.

were required, which means that gas dispersion always operated under laminar flow conditions.

The key information collected for the foamy fluids in this work are, namely, the void fraction, the bubble size distribution and the rheological properties. The void fraction was measured using density measurements, applied to the continuous phase (ρ_c) and the foamy fluids (ρ) collected at the outlet of the mixing head, respectively:

$$\phi = 1 - \frac{\rho}{\rho_c} \quad (16)$$

The bubble size distribution was monitored by on-line optical microscopy coupled to image analysis (*Labbafi et al.*, 2007). This involves an Axiovert 25 microscope (*Zeiss GmbH*, Germany) coupled with a CCD camera (*Kappa Opto-Electronics GmbH*, Germany). As bubbles were spherical, image analysis was limited to the estimation of the radius of spherical objects. The Sauter mean radius R_{32} , *i.e.* the surface-average bubble radius, was deduced by averaging the data, using more than 500 bubbles for each set of operating conditions. The rheological properties were obtained from flow and oscillatory shear testing using a stress-controlled rheometer

(AR-G2 from *TA Instruments*, USA). All the density and rheological measurements were carried out in triplicate. For flow curves, the shear stress (τ) and the viscosity (η) were monitored at 20°C for shear rate values ($\dot{\gamma}$) between 10^{-2} and 10^3 s^{-1} using a parallel plate geometry and a Peltier system for temperature control. Steady state sweep tests were applied. Normal force could also be measured but for parallel plate, this gives access to the difference between the primary and the secondary normal stress differences ($N_1 - N_2$). For dynamic oscillatory measurements, preliminary strain sweep tests at 1 Hz frequency were carried out. Mechanical spectra were, therefore, recorded at a constant strain of 2% for frequency between 0.01 and 10 Hz. Complex (G^*), storage (G') and loss (G'') viscoelastic moduli were monitored together with the complex viscosity (η^*). As the maximum bubble diameter measured in this work was lower than 50 μm , a 1 mm gap was used for steady and oscillatory tests, which was sufficient to prevent confinement effects and to maintain the structure of the foamy fluid during the setup procedure on the plate of the rheometer. Similarly, wall slip was never observed because of the sticky character of the aqueous solutions of glucose syrup. A thin layer of *n*-hexadecane oil was maintained on the side of the sample so as to prevent the surface crystallization of glucose syrup. The same methodology was applied to the continuous phase and to the foamy fluids, in particular to obtain η_c , and η under similar conditions.

As stability is a prerequisite for rheological testing, the stability of the foamy fluids was investigated using a CCD camera for 3 days (*Kappa GmbH*, Germany). The evolution over time of the height $h(t)$ of the region occupied only by the continuous phase in a beaker initially filled up with foam was recorded in this period. This was sufficiently large (5 cm diameter) in comparison to bubbles (about 50 μm diameter) to avoid wall effects. All the measurements were done threefold for statistical purpose.

3 STABILITY OF FOAMY FLUIDS

As mentioned above, stability is a prerequisite, first when the foamy fluid will be used for subsequent experiments, particularly rheological testing but also for any further use. Bubble creaming and liquid drainage appeared to be the main destabilizing mechanisms, while coalescence remained negligible in the first 24 hours, as shown in [Figure 4](#). In this period, a destabilization parameter (S) could be defined as a percentage, *i.e.* as the normalized height $h(t)/h_0$ occupied by the liquid region in the beaker. Consequently, this parameter increases when

destabilization proceeds. As the height of the beaker was $h_0 = 35 \text{ mm}$, [Figure 4](#) after 24 hours illustrates that a few hours of stability against creaming could be achieved for the foamy fluids. Actually, the evolution of $S(t)$ was shown to be perfectly linear with time in the first 24 hours. This behaviour is illustrated by [Figure 5a](#). This figure also shows that the stability over time of the foamy fluid increased strongly with the void fraction, as the slope of curves decreased when ϕ increased. This could be analysed as a hindrance effect, but quantitative analysis is required before making final conclusions.

It is known that the terminal rise velocity of a bubble may either increase or decrease when the void fraction increases. When the terminal rise velocity decreases, this is due to a hindrance effect similar to a “crowding” effect; when it decreases, this is usually attributed to a drag reduction due to bubble wakes which operates as a cooperative effect. Also, a transition between hindered and cooperative rise has often been reported in bubbly flows in the air/water system at increasing ϕ values ([Roghair et al., 2011](#)). More precisely, cooperative rise usually results from the aspiration of small bubbles in the wake of larger bubbles. One of the most popular approaches that accounts for this transition has been proposed by Richardson and Zaki in the 50s, but for spherical particles, a versatile model has been proposed by [Barnea and Mizrahi \(1973\)](#). These authors have applied a “mean field” approach in which a bubble is considered as a single particle which is rising in a pseudo-homogeneous bubbly suspension, the density and the viscosity of which are the density and the viscosity of the pseudo-homogeneous medium. In practise, they used for η a model that approaches Equation (5b). Finally, the Barnea-Mizrahi equation is expressed as follows:

$$\frac{dh}{dt} = v_b = \underbrace{\frac{\Delta\rho \cdot g \cdot d_{43}^2}{18\eta_c}}_{v_\infty} \cdot \frac{(1-\phi)^2}{(1+k_B \cdot \phi^{1/3})} \cdot \exp\left(-\frac{5\phi}{3(1-\phi)}\right) \quad (17)$$

in which v_∞ corresponds to the terminal rise velocity of a single bubble given by the Stokes equation and k_B is a constant that measures the intensity of the crowding effect. As expected, v_∞ depends only on the viscosity and the density of the continuous phase and on the volume-average bubble diameter (d_{43}) deduced from image analysis in this work. The conventional $k_B = 1$ value from Barnea and Mizrahi for solid particles always predict a hindrance effect. In this work, k_B was adjusted by fitting experimental data. A slightly negative value was obtained, which predicted a cooperative rise that was

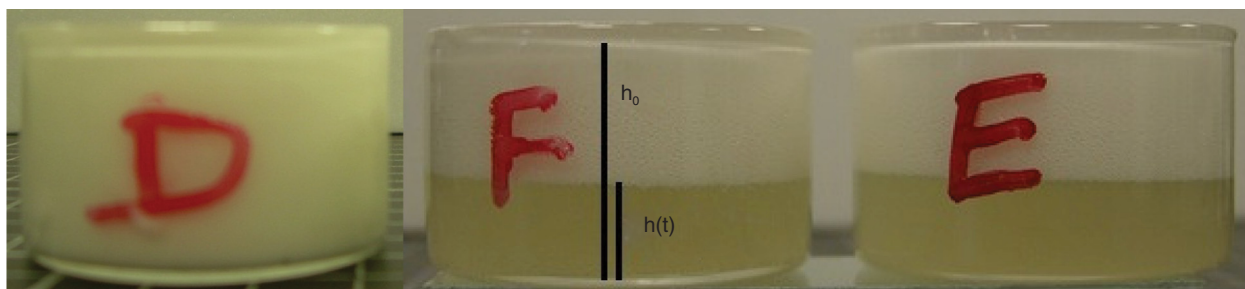


Figure 4

Examples of foamy fluids destabilized by creaming after 24 hours ($\eta_c = 1.3$ Pa.s): D, $t = 0$; E and F, $t = 24$ h, samples compared for testing reproducibility.

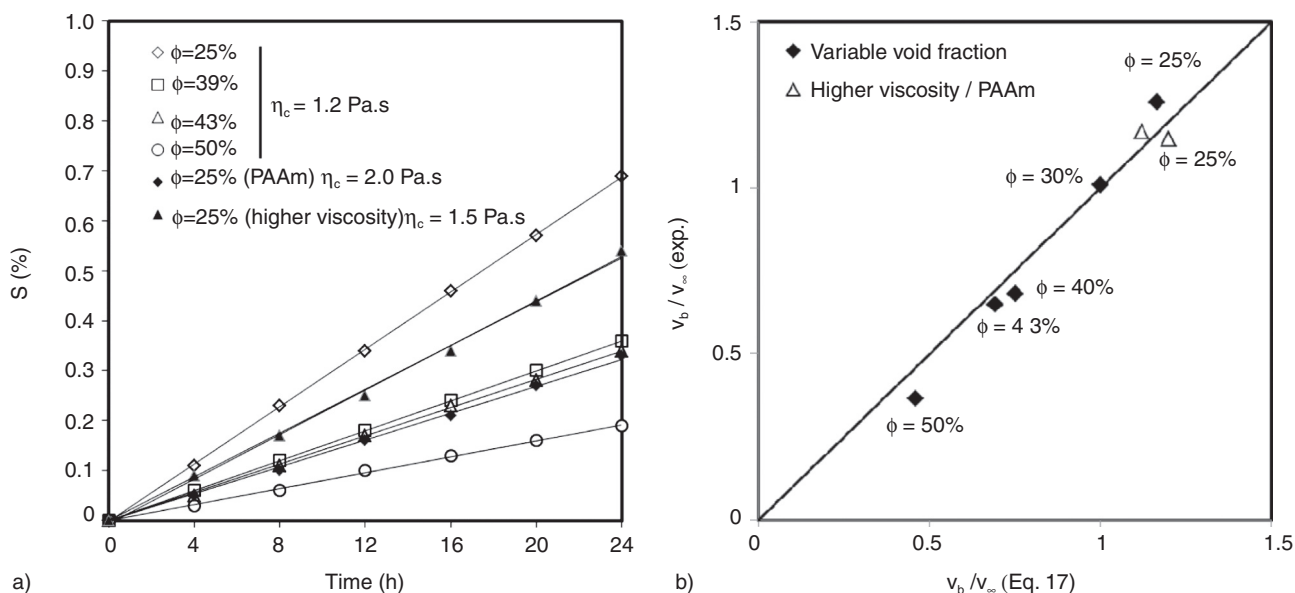


Figure 5

a) Influence of ϕ , η_c and PAAm addition on the stability of the foamy fluid over time. b) Comparison of Equation (17) with experimental data.

limited to $\phi < 30\%$. Figure 5b shows the very good agreement between Equation (17) and experimental data, with a regression coefficient $R^2 = 0.95$ for the fitting plot $y = x$. The cooperative rise was observed for $\phi = 25\%$, i.e. when $v_b/v_\infty > 1$, while hindered rise prevailed for higher ϕ values with a transition about 30%. This kind of transition had already been observed in aerated food and reported by Dickinson (1992), even though it remains scarce in the literature. In the present work, the effect of the cooperative effect remains weak, limited to void fractions between 25% and 30%. In this

region, a possible explanation is that bubble rise is mainly driven by the largest bubbles and not by the bubbles of average diameter, which fits a small cooperative rise effect (10-15% above the single bubble velocity). Then, when void fraction increases, the hindrance effect starts dominating because the bubble size distribution does not change significantly, while the hindrance effect is enhanced by ϕ , which could explain the limited range of cooperative rise. However, this analysis is difficult to validate quantitatively because of the limited range of ϕ value in which cooperative rise is reported.

In parallel, Figure 5b highlights that Equation (17) takes correctly into account the influence of η_c that emerges from Figure 5a. Consequently, the effect of composition may be used to slow down creaming, for example the addition of PAAm at constant glucose syrup content, but less than expected because the increase of η_c may be partially counterbalanced by an increase of bubble size due to viscoelasticity. For a limited addition, Figure 5b shows that increasing elasticity with PAAm had no significant effect on the stability of the foamy fluid and that η_c always played the key role, as Equation (17) does not account for elasticity. Finally, Figure 5b highlights that the preliminary analysis of Figure 5a was incomplete and that the increased stability of the foamy fluids at increasing ϕ values hid a transition between two different regimes of cooperative and hindered rises.

As a conclusion, experimental results showed that stable foamy fluids could be prepared with a gas fraction between 25% and 50% (v/v) by varying air flow rate. For $\eta_c = 1.2$ Pa.s, experiments showed that this result could be extended to $\phi = 55\%$. Rheological measurements using 1 mm gap may be carried out, provided the experiments remain within 10-15 min time limit, but under process conditions, these model fluids could be used to simulate other kinds of foamy fluids for several hours. This stability results not only from the viscosity of the matrix but also from the small bubble size. Image analysis showed, indeed, that bubble size distributions were monomodal, with Sauter radii between 7 and 20 μm as a function of rotation speed in the mixer, and that they exhibited reduced polydispersity. This was confirmed by the ϕ_m values deduced from Equation (6) which were all around 0.65, very close from the theoretical value of 0.637 and significantly lower than the 0.7 value used by Pal (2003) to fit the experimental data reported by Rust and Manga (2002). A remaining question concerns the extent of the change of R_{32} on the results observed in Figure 5a. Actually, experimental results demonstrated that bubble size and polydispersity were slightly reduced when rotation speed increased, as already shown in Narchi *et al.* (2011). In this work, Figure 6 also highlights that R_{32} and polydispersity do not change significantly with ϕ when rotation speed was higher than 400 rpm. Finally, it can be concluded that ϕ and R_{32} can be considered as independent variables with the continuous manufacturing process used in this work.

However, at longer times than 24 hours, the analysis of the stability of the foamy fluid was impeded by the problem of surface crystallization of glucose syrup due to local evaporation at the air/water interface. The interpretation of experimental data became, therefore, more

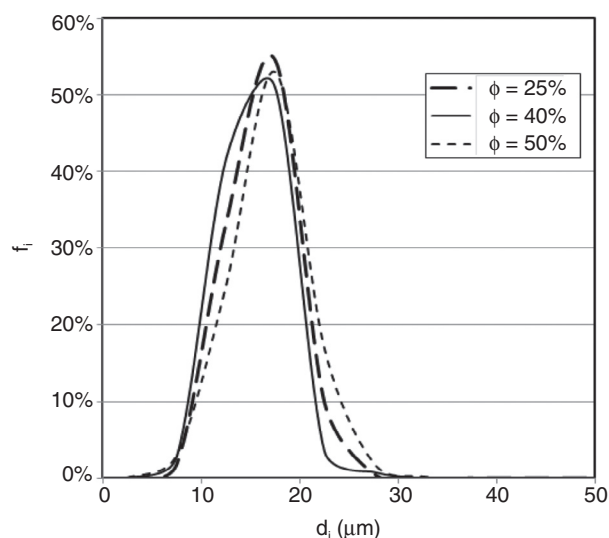


Figure 6

Example of bubble size distributions at several ϕ values in the foamy fluids without PAAm at a rotation speed of 1000 rpm.

complex, but coalescence still seemed to remain negligible. As a result, the analysis of the stability with continuous phases of higher viscosity than $\eta_c = 1.2$ Pa.s was biased even more rapidly by surface crystallization due to the increased amount of glucose syrup. Consequently, it will be supposed in this work that the trends observed in Figure 5 can be extended to higher viscosity fluids, although their experimental validation becomes more difficult.

4 RHEOLOGY OF FOAMY FLUIDS UNDER CONTINUOUS SHEAR FLOW

Using stability data, rheological testing procedures were defined, with experiments of about 15 min and a 1 mm gap to avoid bubble creaming. First, the rheological properties of the foamy fluids were investigated under flow conditions. As expected, foamy fluids displayed a viscoelastic fluid behavior under shear flow with non-zero normal stress difference even when the continuous phase was Newtonian. The viscosity (η) of the foamy fluids could also be lower than the viscosity as the continuous phase (η_c), as already reported in the literature. The evolution of η was shown to result from the interplay between the formulation of the continuous phase, void fraction and bubble size. For all the mixtures, foamy fluids always exhibited a zero-shear Newtonian plateau

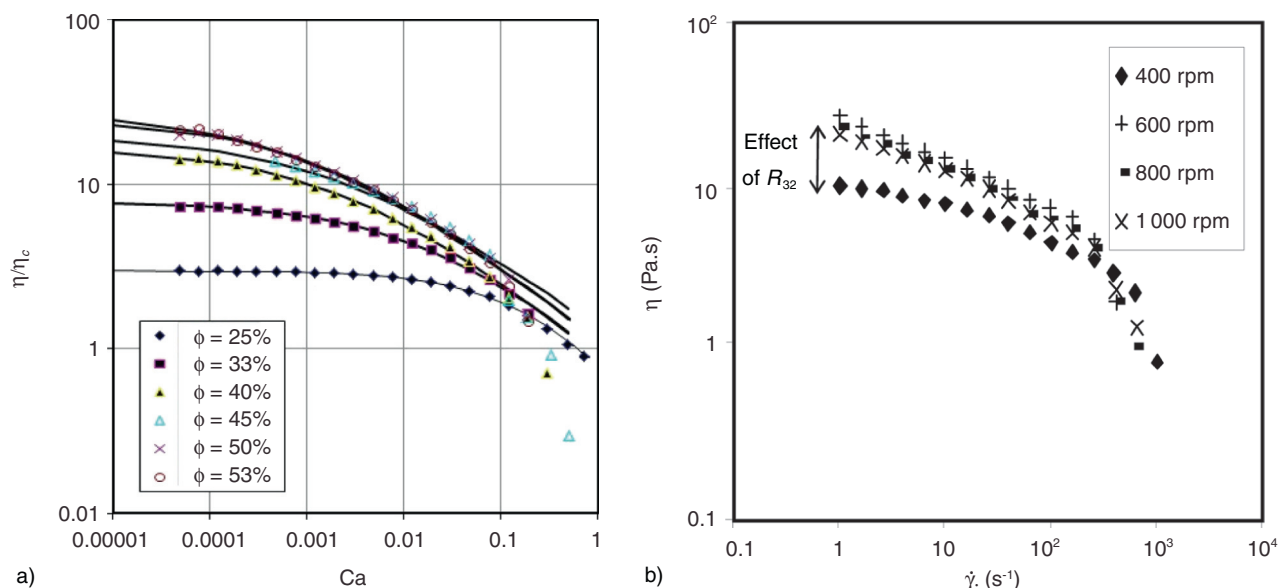


Figure 7

a) Evolution of relative viscosity (η/η_c) as a function of ϕ . Lines correspond to the fitted data obtained by adjusting Equation (8).
 b) Evolution of the flow curve as a function of the rotation speed used to prepare the foamy fluids for $\phi = 40\%$.

region η_0 , regardless the continuous phase contained PAAm or not. Void fraction appeared to have the most significant effect, as shown in Figure 7a: η_0 increased with ϕ in Figure 7a when R_{32} was constant (Fig. 6). This agrees qualitatively with literature data (Rust and Manga, 2002; Llewellyn *et al.*, 2002) and with most of the models described in section 2 and in Figure 2. No infinite-shear plateau was observed, as expected for fluids with $\eta_c < 10$ Pa.s. On the contrary, η_0 values were more accurately determined from the curves than with more viscous continuous phases, at least up to $\phi = 40\%$ (Llewellyn *et al.*, 2002). Also, the upper limit of the zero-shear plateau region in terms of Ca decreased rapidly when void fraction increased in Figure 7a: from $Ca \approx 0.1$ at when $\phi = 25\%$ to $Ca < 10^{-4}$ for $\phi = 50\%$, which confirms the key role of the void fraction on the rheology of the foamy fluids. It seems that increasing the interactions between bubbles under flow conditions enhanced the non-Newtonian behaviour of the foamy fluid, in agreement with the literature on emulsions.

Quantitatively, the apparent viscosity η could be adequately described using the Cross equation (Eq. 8), as illustrated by Figure 7a. This result is in qualitative agreement with Rust and Manga (2002) but the values of their fitted parameters strongly differed with those of this work, in particular the exponent m which was higher than 1 in their data. This may result from the fact

that when η varies significantly with Ca , two regions could be distinguished:

- a conventional shear-thinning region in which bubbles may be deformed reversibly and in which the relative viscosity η/η_c may be lower than 1 at high shear, for example for $\phi = 25\%$ in Figure 7a;
- a region in which the viscosity falls or cannot be measured because the microstructure of the foamy fluid is irreversibly broken, probably by bubble coalescence. This occurs usually at Ca values just higher than 0.1-0.2, except when $\phi = 25\%$ at which the probability of bubble collision is lower. This value corresponds roughly to the critical dimensionless stress for breakup $(\eta\dot{\gamma}R_{32})\sigma$ in wet foams estimated by Golemanov *et al.* (2008) in the presence of surfactants but further work is still needed to confirm if this value can be extended to protein-stabilized foamy fluids.

The precise limit between the two regions is difficult to estimate accurately in practice. Theoretically, the method consists in applying the same shear rate sweep test after appropriate rest on a sample. In practice, experimental results could be impaired by the reduced stability of the foamy fluid due to bubble creaming and liquid drainage: this was the reason why flow curves experiments were limited to 15 min. As a result, the limit of the first region was considered, as a rough approximation, to be the maximum shear rate at which

reproducible data could be obtained on different samples in this work, as bubble coalescence usually leads to non-reproducible viscosity data.

The exponent of Equation (8) was fitted using only the first region in this work, which gave 0.50 ± 0.05 for all the ϕ values tested. This means that η scales as $Ca^{-1/2}$ when η varies with Ca , *i.e.* that the viscous shear stress (τ) scales as $Ca^{1/2}$. This result is in qualitative agreement with data on wet foams with immobilized interfaces. For these, the wall shear stress consists of a yield stress and a viscous component, while it can be considered that only the second one is observed in foamy fluids. It is commonly admitted in the literature on wet foams that the viscous component scales with $Ca^{2/3}$ for mobile interfaces but with $Ca^{1/2}$ for immobile interfaces that correspond to protein-covered bubble interfaces (Zhao *et al.*, 2009; Politova *et al.*, 2012). The good agreement between foamy fluids and wet foams seems intuitive, as phenomena are similar, especially close to the very wet limit, although the assumptions leading to $\tau \sim Ca^{1/2}$ in wet foams are not valid for foamy fluids. Consequently, this experimental result must still be confirmed by further work.

A remaining question is to know to which extent η_0 and η depend on bubble size. Figure 7b shows that η_0 values decreased when R_{32} increased at constant ϕ , although the influence of R_{32} was smaller than that of ϕ .

In this figure, R_{32} decreased from 14 to 10 μm due to the increase of rotation speed from 400 to 600 rpm, and then, it became nearly constant for a further increase of rotation speed with $\phi = 40\%$. Similarly, the extent of the zero-shear viscosity plateau appeared to be reduced when bubble size decreased, *i.e.* using higher rotation speed (Fig. 7b). Actually, a similar effect could be observed by acting on the recipe: the addition of 0.01% (w/v) PAAm gave a slightly shear-thinning behaviour to the matrix that could be retrieved in the foamy fluids (data not shown). This can explain the discrepancy between literature data on η_0 , as shown by Figure 2a: all the models presented do not account for R_{32} and polydispersity, while these parameters affect η_0 , probably because of the increased interfacial interactions between spherical bubbles when R_{32} decreases at constant ϕ .

In Figure 8a, η_0 values were shown to be predicted accurately using a Mooney equation with $\alpha = 1$ as a function of void fraction up to 40% but this model strongly overpredicted η_0 for ϕ values between 45% and 55%. The best fit below 40% was obtained by optimizing ϕ_m about 0.62, which remains close to the theoretical value. This also indicated that models corresponding to Equations (9-11) were not able to describe adequately the $\eta(Ca)$ curves. Experimental η/η_c values also appeared to be higher than most of

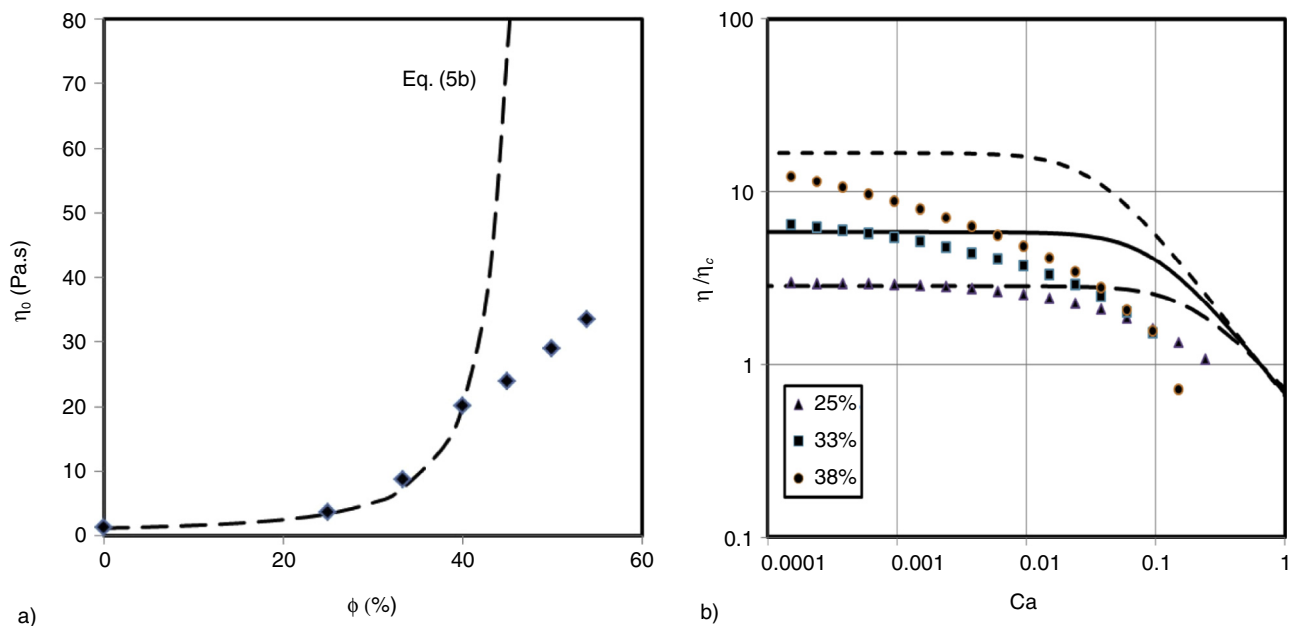


Figure 8

a) Evolution of zero-shear viscosity (η_0) as a function of void fraction ϕ . b) Comparison between Equation (14) coupled to Equation (5b) for η_0 with experimental data.

those reported in the literature on foamy fluids. Four obvious reasons may explain these different trends:

- first, η_0 values obtained for $\phi \geq 40\%$ are only adjusted values, as the zero-shear plateau is not reached in [Figure 7a](#). As a result, they could be underestimated, which could explain the change of behaviour observed in [Figure 8a](#) above 40% void fraction;
- η values become increasingly sensitive to ϕ when it approaches ϕ_m . Consequently, the uncertainty on η_0 , especially due to the sampling and the set up procedures, should increase with ϕ ;
- contrary for example to [Llewelin et al. \(2002\)](#), a surface-active agent is used in this work, which modifies the rigidity of the interface. This is the reason why the $\alpha = 1$ value used for η_0 is in line with the conclusions reported on the $Ca^{1/2}$ behaviour, as they both describe rigidified interfaces. This could explain the differences with literature data. In addition, it must be pointed out that the rigid and mobile approximations for interfaces constitute only rough estimations between which viscosity may vary continuously as far as mobility can be modified. Although proteins have been used in excess, interface rigidity may vary when ϕ increases and a slight change of interface mobility may dramatically affect the viscosity, as shown by [Pal \(2011\)](#) for concentrated emulsions;
- finally, the last reason that could explain the differences with literature data is that bubble diameters were about one order of magnitude larger in this work than in [Llewelin et al. \(2002\)](#). Actually, it is well known for emulsions that viscosity depends on droplet size because of the increase of surface area on which the internal friction between particles applies ([Pal, 1998](#)). The same should also apply for the foamy fluids. As already mentioned for η_0 , it is probable that this last point mainly explains the variability between the $\eta(Ca)$ curves of foamy fluids in the literature.

On the basis of the analysis of [Figure 8a](#), only Equation (14) with a viscosity function based on the Mooney equation ([Eq. 5b](#)) was tested against experimental data for fitting $\eta(Ca)$ curves. However, this approach was not able to predict correctly the shear-thinning behaviour of foamy fluids, especially the upper limit of the zero-shear viscosity region ([Fig. 8b](#)). This limit in terms of shear rate or Ca appeared to decrease more rapidly than predicted by Equation (14) in [Figure 8b](#), which is in line with the rapid increase of the fitted k_C value in Equation (8): from 2×10^{-3} for $\phi = 25\%$ to 0.3 for $\phi = 50\%$. This parameter seems to follow an exponential increase but additional data are compulsory before it can be correctly fitted.

As a conclusion, first-order models based on a theoretical analysis of bubble deformation fail to predict

the experimental results. Only the semi-empirical Cross model is able to describe $\eta(Ca)$ curves, with a η_0 value predicted by means of the Mooney equation up to $\phi = 40\%$. This confirms that void fraction is the key parameter acting on the viscosity of the foamy fluid but also that bubble size R_{32} and polydispersity also affect η , which is scarcely accounted for in the literature. As expected from literature data, the behavior of foamy fluids seems to be closer to those of concentrated polydisperse suspensions or emulsions than to foams, except that viscosity falls below η_c . However, the $Ca^{1/2}$ behaviour observed in the shear-thinning region when coalescence does not occur highlights that some of the models able to describe wet foams could be applied in the future. This could improve the theoretical description of the shear-thinning region in which only empirical models such as the Cross equation can be used, as already pointed by [Rust and Manga \(2002\)](#) ten years ago. In this work, the main advantage of the continuous process used to prepare foamy fluids is, finally, that it ensures a reproducible monomodal and narrow bubble size distribution independent of ϕ . This may be valuable to investigate the behaviour of foamy fluids under process conditions, as the rheology can be tuned and the impact of both effects can be distinguished.

5 ANALYSIS OF THE VISCOELASTIC CHARACTER OF FOAMY FLUIDS

The foamy fluids were subjected to oscillatory testing procedures. First, strain sweep tests were applied so as to estimate the limit of the linear viscoelastic region. These showed that G' and G'' were nearly constant, which corresponded to fluid materials but also that phase angle δ was between 75° and 85° at 1 Hz, which highlighted a slightly viscoelastic behavior. This was in agreement with frequency sweep tests: tangent loss $\tan \delta$ was always between 1.5 and 10 in at 2% strain ([Fig. 9a](#)). The viscoelastic character of fluids could only be enhanced by adding 0.01% (w/v) PAAm in the recipe. In this case, $\tan \delta$ could approach 1 (data not shown). These results show that these materials were foamy fluids; they differed from wet foams because they exhibited no yield stress and were slightly viscoelastic even when the continuous phase was Newtonian because of the interactions between bubbles.

However, the above-mentioned behaviors are reported at low shear, whereas bubble deformation should promote the development of the elastic character of the foamy fluid at high shear. This is highlighted by the evolution of the estimation of the primary normal stress difference N_1 in [Figure 9b](#) under flow conditions:

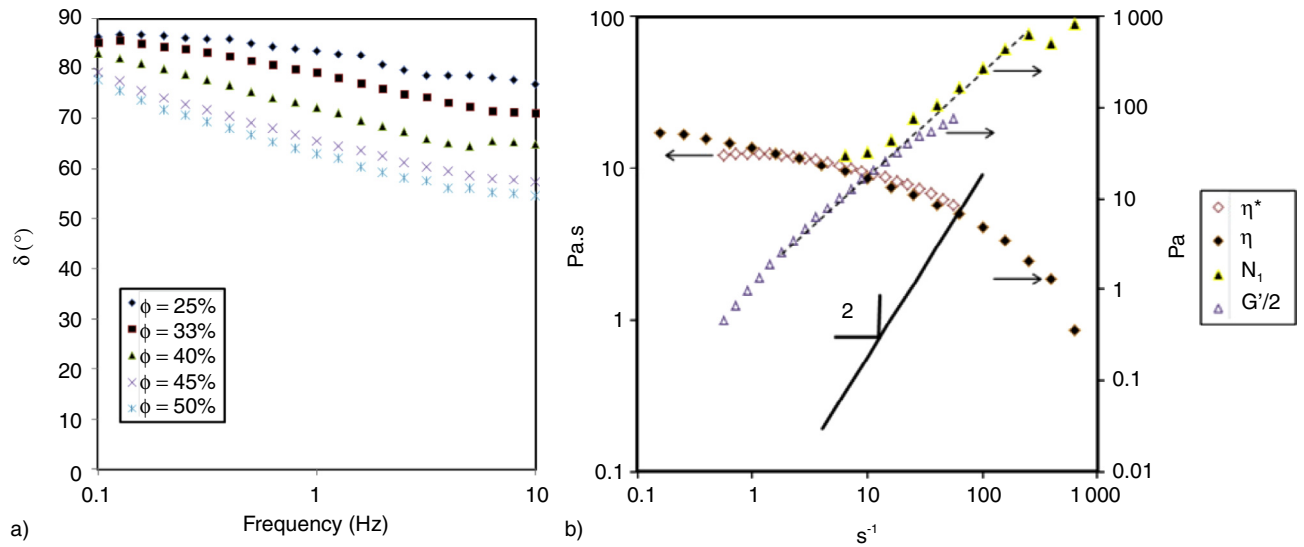


Figure 9

a) Evolution of the phase angle δ with frequency and ϕ in mechanical spectra at 2% strain. b) Example of validation of the Cox-Merz and Laun's rules at 2% strain ($\phi = 40\%$).

N_1 could be measured only when the shear rate is higher than 10 s^{-1} for $\phi \geq 40\%$. In this work, N_1 was estimated using qualitatively from Equation (12), as the parallel plate geometry gives access to experimental $N_1 - N_2$ values. Contrary to polymer solutions for which $|N_2| \ll N_1$ in general, Eq. (12) shows that $|N_2|$ approaches $N_1/2$ at low Ca. This assumption was applied to deduce N_1 from $N_1 - N_2$ data. Even though N_1 was shown to increase with ϕ at constant R_{32} value, the reduced range of void fractions at which N_1 could be estimated ($40\% \leq \phi \leq 50\%$) did not enable to develop a model for $N_1(\phi)$. A key problem was also that Equation (12) was unable to predict quantitatively N_1 values in this work: it predicts a slope close to 2 in Figure 9b, while the slope is close to 1 in practice. Further work is, therefore, needed to confirm the validity of the assumption $|N_2| = N_1/2$. An indication that this assumption may be valid is that not only the Cox-Merz rule was shown to apply for ϕ values between 25% and 50% but also the Laun's rule. The Cox-Merz rule postulates that the complex viscosity η^* from mechanical spectra and the viscosity η from flow curves can be confounded, while the Laun's rule assumes that the storage modulus G' and N_1 can be related at low shear by $G'/2 = N_1$. Their applicability was, however, limited to Ca values below 0.1 for foamy fluids in Figure 9b. In the literature, the empirical Cox-Merz rule is usually applied to extend viscosity data at low shear rate using oscillatory testing.

For foamy fluids, this is constrained by the time limit that does not give access to low frequency data. Conversely, the advantage is that the Laun's rule could be easily used to extend N_1 at lower ϕ and shear rate values, provided the $|N_2| = N_1/2$ assumption is validated.

As a conclusion, a more comprehensive description of the rheological properties of the foamy fluids has been obtained. Up to now, experimental data on the viscoelastic properties of foamy fluids using oscillatory testing remained scarce in the literature and no data could be found on N_1 as far as the authors know. Similarly, the applicability of the Cox-Merz rule had not been reported. The applicabilities of Cox-Merz and Laun's rules for foamy fluids constitute, therefore, key results because they allow the comparison between low and high shear testing conditions, *i.e.* the comparison between data from rheometers with those from process conditions. Consequently, a better understanding of the viscoelastic properties of foamy fluids is expected in the future so as to better predict their behaviour in the process industries.

CONCLUSION

In this work, the properties of a model foamy fluid based on glucose syrup solutions and whey proteins as foaming promoters have been studied. This model fluid can be

prepared easily with reproducible and tuneable properties, using a continuous process under steady state conditions. These foamy fluids exhibit a stability of several hours at rest and can be sheared up to Ca about 0.1 (*i.e.* about 100 s^{-1}) without impairing their microstructure. Also, their stability over time has been modelled quantitatively as a function of void fraction. These foamy fluids constitute, therefore, an adequate model fluid to investigate under process conditions the behaviour of real foamy fluids that can be found, for example, in the food and the oil industries. For example, in the oil industry, they could be used to model the behaviour of foamy oil as they can be studied under various pressures, except that they do not account for bubble nucleation. Another key advantage is that the void fraction of these model fluids can be varied between 25% and 50%, while the bubble size distribution remains nearly unchanged, which enables to investigate the influence of void fraction independently from bubble size.

In this work, the applicability and the limits of the most common viscosity models from the literature have also been analysed. A key conclusion is that the rheological properties of foamy fluids depend strongly on void fraction but also on bubble size. Consequently, they can be compared as a function of ϕ only for similar bubble size distributions. On the viscosity of foamy fluids, this work has shown that only semi-empirical models could correctly fit the flow curves. On the contrary, an important theoretical finding is that in the shear-thinning region, viscosity was shown to vary as $Ca^{-1/2}$, as for wet foams. Further work will be devoted to determine whether it is possible to relate theoretically the viscosity of the foamy fluids to that of wet foams. Similarly, the applicability of the Cox-Merz and Laun's rules constitutes a key improvement, in particular to investigate the viscoelastic properties of foamy fluids as a function of ϕ under flow conditions. These have been disregarded up to now, although they are intrinsically linked to bubble deformation. In particular, Laun's rule will be valuable because it can be used to link viscoelastic properties under oscillatory conditions to those under process conditions. This will be also the subject of further work. In the future, we hope that the information deduced from the comparison with wet foams and from the applicability of Laun's rule will give access to a better understanding and modelling of the behaviour of foamy fluids when they are encountered in the process industries.

REFERENCES

- Abivin P., Hénaut I., Argillier J.-F., Moan M. (2009) Rheological behavior of foamy oils, *Energy Fuels* **23**, 3, 1316-1322.
- Ahmed R.M., Takach N.E., Khan U.M., James S., Saasen A., Godoy R. (2009) Rheology of foamed cement, *Cem. Concr. Res.* **39**, 4, 353-361.
- Barnea E., Mizrahi J. (1973) A generalized approach to the fluid dynamics of particulate systems: Part 1. General correlation for fluidization and sedimentation in solid multiparticle systems, *Chem. Eng. J.* **5**, 2, 171-189.
- Berli C.L.A., Quemada D. (2000) Prediction of the interaction potential of microgel particles from rheometric data. Comparison with different models, *Langmuir* **16**, 26, 10509-10514.
- Camarasa E., Vial C., Poncin S., Wild G., Midoux N., Bouillard J. (1999) Influence of coalescence behaviour of the liquid and of gas sparging on hydrodynamics and bubble characteristics in a bubble column, *Chem. Eng. Process.* **38**, 4-6, 329-344.
- Chaumat H., Billet A.M., Delmas H. (2007) Hydrodynamics and mass transfer in bubble columns: Influence of liquid phase surface tension, *Chem. Eng. Sci.* **62**, 24, 7378-7390.
- Choi S.J., Schowalter W.R. (1975) Rheological properties of nondilute suspensions of deformable particles, *Phys. Fluids* **18**, 4, 420-427.
- Denkov N.D., Subramanian V., Gurovich D., Lips A. (2005) Wall slip and viscous dissipation in sheared foams: Effect of surface mobility, *Colloids Surf. A: Physicochem. Eng. Aspects* **263**, 1-3, 129-145.
- Denkov N.D., Tcholakova S.S., Höhler R., Cohen-Addad S. (2012) Foam Rheology (Chap. 6), in *Foam Engineering: Fundamentals and Applications*, Stevenson P. (ed.), John Wiley & Sons, Chichester, UK.
- Derkach S.R. (2009) Rheology of emulsions, *Adv. Colloid Interface Sci.* **151**, 1-2, 1-23.
- Dickinson E. (1992) *An Introduction to Food Colloids*, Oxford University Press, New York.
- Ekambara K., Sanders R.S., Nandakumar K., Masliyah J.H. (2008) CFD simulation of bubbly two-phase flow in horizontal pipes, *Chem. Eng. J.* **144**, 2, 277-288.
- Golemanov K., Tcholakova S., Denkov N.D., Ananthapadmanabhan K.P., Lips A. (2008) Breakup of bubbles and drops in steadily sheared foams and concentrated emulsions, *Phys. Rev. E* **78**, 051405.
- Gourich B., Vial Ch, Belhaj Soulamy M., Zoulalian A., Ziyad M. (2008) Comparison of hydrodynamic and mass transfer performances of an emulsion loop-venturi reactor in cocurrent downflow and upflow configurations, *Chem. Eng. J.* **140**, 1-3, 439-447.
- Herzhaft B. (1999) Rheology of aqueous foams: a literature review of some experimental works, *Oil Gas Sci. Technol.* **54**, 5, 587-596.
- Hibiki T., Lee T.H., Lee J.Y., Ishii M. (2006) Interfacial area concentration in boiling bubbly flow systems, *Chem. Eng. Sci.* **61**, 24, 7979-7990.
- Hotrum N.E., Cohen Stuart M.A., van Vliet T., Avino S.F., van Aken G.A. (2005) Elucidating the relationship between the spreading coefficient, surface-mediated partial coalescence and the whipping time of artificial cream, *Colloids Surf. A: Physicochem. Eng. Aspects* **260**, 1-3, 71-78.
- Jakubczyk E., Niranjana K. (2006) Transient development of whipped cream properties, *J. Food Eng.* **77**, 1, 79-83.
- Jung D.-M., Ebeler S.E. (2003) Investigation of binding behavior of α - and β -ionones to β -lactoglobulin at different pH values using a diffusion-based NOE pumping technique, *J. Agric. Food Chem.* **51**, 7, 1988-1993.

- Labbafi M., Thakur R.K., Vial C., Djelveh G. (2007) Development of an on-line optical method for assessment of the bubble size and morphology in aerated food products, *Food Chem.* **102**, 2, 454-465.
- Llewellyn E., Manga M. (2005) Bubble suspension rheology and implications for conduit flow, *J. Volcanol. Geothermal Res.* **143**, 1-3, 205-217.
- Llewellyn E.W., Mader H.M., Wilson S.D.R. (2002) The rheology of a bubbly liquid, *Proc. R. Soc Lond. A* **458**, 2020, 987-1016.
- Marinova K.G., Basheva E.S., Nenova B., Temelska M., Mirarefi A.Y., Campbell B., Ivanov I.B. (2009) Physico-chemical factors controlling the foamability and foam stability of milk proteins: Sodium caseinate and whey protein concentrates, *Food Hydrocoll.* **23**, 1864-1876.
- Murray B.S., Durga K., Yusoff A., Stoyanov S.D. (2011) Stabilization of foams and emulsions by mixtures of surface active food-grade particles and proteins, *Food Hydrocoll.* **25**, 4, 627-638.
- Narchi I., Vial C., Djelveh G. (2009) Effect of matrix elasticity on the continuous foaming of food models, *Appl. Biochem. Biotechnol.* **151**, 2-3, 105-121.
- Narchi I., Vial C., Labbafi M., Djelveh G. (2011) Comparative study of the design of continuous aeration equipment for the production of food foams, *J. Food Eng.* **102**, 2, 105-114.
- Pal R. (1998) A novel method to correlate emulsion viscosity data, *Colloids Surf. A: Physicochem. Eng. Aspects* **137**, 1-3, 275-286.
- Pal R. (2003) Rheological behavior of bubble-bearing magmas, *Earth Planet. Sci. Lett.* **207**, 1-4, 165-179.
- Pal R. (2006) *Rheology of Particulate Dispersions and Composites*, CRC Press, Boca Raton.
- Pal R. (2011) Influence of interfacial rheology on the viscosity of concentrated emulsions, *J. Colloid Interface Sci.* **356**, 1, 118-122.
- Politova N., Tcholakova S., Golemanov K., Denkov N.D., Vethamuthu M., Ananthapadmanabhan K.P. (2012) Effect of cationic polymers on foam rheological properties, *Langmuir* **28**, 2, 1115-1126.
- Roghair I., Lau Y.M., Deen N.G., Slagter H.M., Baltussen M.W., VanSint Annaland M., Kuipers J.A.M. (2011) On the drag force of bubbles in bubble swarms at intermediate and high Reynolds numbers, *Chem. Eng. Sci.* **66**, 14, 3204-3211.
- Rust A.C., Manga M. (2002) Effects of bubble deformation on the viscosity of dilute suspensions, *J. Non-Newtonian Fluid Mech.* **104**, 1, 53-63.
- Ruzicka M.C., Drahoš J., Mena P.C., Teixeira J.A. (2003) Effect of viscosity on homogeneous-heterogeneous flow regime transition in bubble columns, *Chem. Eng. J.* **96**, 1-3, 15-22.
- Saint-Jalmes A., Durian D.J. (1999) Vanishing elasticity for wet foams: Equivalence with emulsions and role of polydispersity, *J. Rheol.* **43**, 6, 1411-1422.
- Thakur R.K., Vial C., Djelveh G. (2008) Effect of composition and process parameters on elasticity and solidity of foamed food, *Chem. Eng. Process.* **47**, 3, 474-483.
- Vinckier I., Minale M., Mewis J., Moldenaers P. (1999) Rheology of semi-dilute emulsions: viscoelastic effects caused by the interfacial tension, *Colloids Surf. A: Physicochem. Eng. Aspects* **150**, 1-3, 217-228.
- Wang J., Yuan Y., Zhang L., Wang R. (2009) The influence of viscosity on stability of foamy oil in the process of heavy oil solution gas drive, *J. Petrol. Sci. Eng.* **66**, 1-2, 69-74.
- Weaire D. (2008) The rheology of foam, *Curr. Opin. Colloid Interface Sci.* **13**, 3, 171-176.
- Weaire D., Hutzler S. (1999) *The Physics of Foams*, Clarendon Press, Oxford.
- Yaron I., Gal-Or B. (1972) On viscous flow and effective viscosity of concentrated suspensions and emulsions. Effect of particle concentration and surfactant impurities, *Rheol. Acta* **11**, 3-4, 241-252.
- Zhao J., Pillai S., Pilon L. (2009) Rheology of colloidal gas aphrons (microfoams) made from different surfactants, *Colloids Surf. A: Physicochem. Eng. Aspects* **348**, 1-3, 93-99.

Manuscript accepted in February 2013

Published online in August 2013

Copyright © 2013 IFP Energies nouvelles

Permission to make digital or hard copies of part or all of this work for personal or classroom use is granted without fee provided that copies are not made or distributed for profit or commercial advantage and that copies bear this notice and the full citation on the first page. Copyrights for components of this work owned by others than IFP Energies nouvelles must be honored. Abstracting with credit is permitted. To copy otherwise, to republish, to post on servers, or to redistribute to lists, requires prior specific permission and/or a fee: Request permission from Information Mission, IFP Energies nouvelles, fax. +33 1 47 52 70 96, or revueogst@ifpen.fr.